Chapter 15
Visual Guidance of an Active Handheld Microsurgical Tool

Brian C. Becker, Sandrine Voros, Robert A. MacLachlan, Gregory D. Hager, and Cameron N. Riviere

Abstract In microsurgery, a surgeon often deals with anatomical structures of sizes that are close to the limit of the human hand accuracy. Robotic assistants can help to push beyond the current state of practice by integrating imaging and robot-assisted tools. This paper demonstrates control of a handheld tremor reduction micromanipulator with visual servo techniques, aiding the operator by providing three behaviors: "snap-to", motion scaling, and standoff regulation. A stereo camera setup viewing the workspace under high magnification tracks the tip of the micromanipulator and the object being manipulated. Individual behaviors are activated in task-specific situations when the micromanipulator tip is in the vicinity of the target. We show that the snap-to behavior can reach and maintain a position at a target with Root Mean Squared Error (RMSE) of 17.5 $\pm$ 0.4 μm between the tip and target. Scaling the operator's motions and preventing unwanted contact with non-target objects also provides a larger margin of safety.

Keywords Medical robotics · Microsurgery · Visual servoing · Machine vision · Tremor · Eye surgery · Vitreoretinal surgery · Micromanipulation · Accuracy

15.1 Introduction

Micromanipulators aid surgical operations by providing extremely precise movements on a small scale. Features such as remote control, force feedback, motion scaling, and virtual fixtures enable advanced behaviors that an unassisted

©2009 IEEE. Reprinted with permission, from Becker, B.C., Voros, S., MacLachlan, R.A., Hager, G.D., Riviere, C.N.: Active guidence of a handheld micromanipulator using visual servoing. In: IEEE International Conference on Robotics and Automation, pp. 339–344 (2009)

C.N. Riviere (✉)
Robotics Institute, Carnegie Mellon University, 5000 Forbes Ave, Pittsburgh, PA 15213, USA
e-mail: camr@ri.cmu.edu

J. Rosen et al. (eds.), *Surgical Robotics: Systems Applications and Visions*,
DOI 10.1007/978-1-4419-1126-1_15, © Springer Science+Business Media, LLC 2011

human would find difficult to replicate. Of particular interest are microsurgery and cell micromanipulation, where very delicate operations must be performed precisely on structures with cross sections varying from millimeters down to microns. Tools like the Steady-Hand [1] help surgeons by suppressing tremor or involuntary hand movement on the order of 50–100 micrometers (μm).

The precision of the surgical gesture and the comfort of the surgeon during the operation can also be improved by exploiting domain-specific knowledge, using preoperative data to design augmented reality systems for biomicroscopy [2, 3] and real-time tracking of surgical instruments and anatomical targets [2] to further improve the precision of the gesture. This information can then incorporate more intelligent behavior into the micromanipulator, such as commanding the tip to reach a target or avoiding anatomical areas that could lead to complications in the surgery. For example, Li et al. [4] derive a controller for gene injection into a 90 μm-diameter oosperm under 100× magnification using a single camera to servo the micro-injector using visual feedback. With a stereo camera setup, the system developed in [5] servos the micromanipulator to inject a sesame seed viewed under a 20× microscope.

Our lab has developed a fully handheld active micromanipulator called Micron whose capabilities include basic tremor suppression and motion scaling [6]. The central problem addressed in this paper is the control of the endpoint of a manipulator to perform tasks relative to an observed point or surface in space. We propose to introduce three behaviors that incorporate domain-specific knowledge and visual feedback to give the surgeon guidance in specific tasks: snap-to, motion scaling, and standoff regulation. One of the main challenges in doing so is that the optical system involved is a microscope: at such high magnifications, the standard calibration techniques commonly used, such as [7], yield unsatisfactory results.

In the remainder of this section, these three behaviors and their workings are explored.

15.2 Background

Micron (Fig. 15.1) is a handheld micromanipulator with piezoelectric actuators built into the handle of the tool. The actuators can position the endpoint, or tip, within a roughly cylindrical workspace 1,500 μm in diameter and 500 μm long. An external measurement system called ASAP (Apparatus to Sense of Position) supplies Micron

Fig. 15.1 Fully handheld active Micron micromanipulator

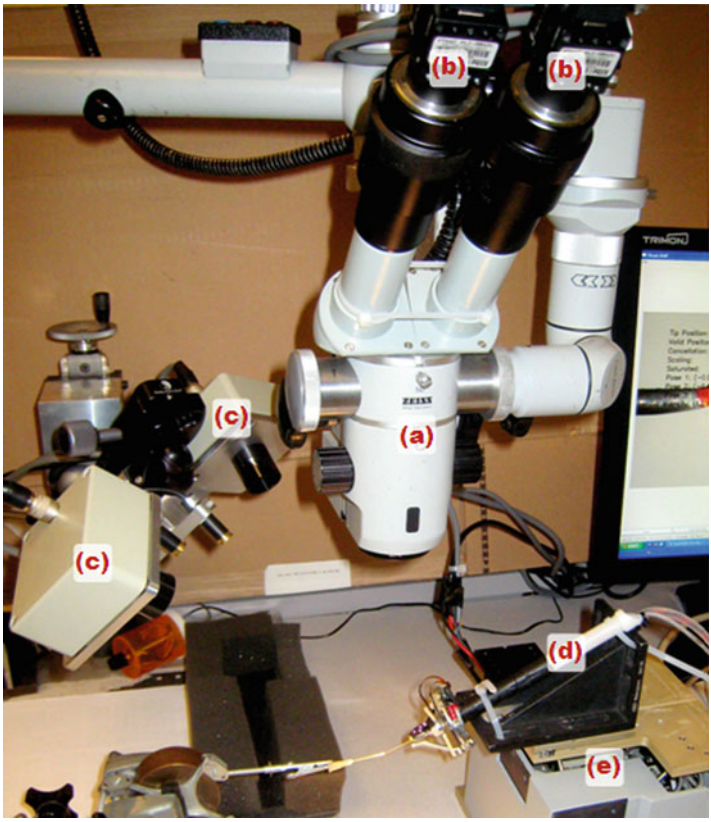

Fig. 15.2 System setup. (**a**) Microscope, *middle center*. (**b**) Cameras, *top right*. (**c**) ASAP measuring sensors, *middle left* (**d**) Micron, *bottom right*, attached to (**e**) Hexapod micropositioner, *lower right*

with real-time position and pose information accurate to $\sim 4 \pm 2$ μm [8]. In addition to the X, Y, and Z location of the Micron tip, a 3×3 rotation matrix defining the pose of the instrument can be obtained. Another useful measurement available is the center position, or where the tip would be nominally pointing if the piezoelectric actuators were not active. ASAP uses position-sensitive detectors (PSD's) to detect four pulsed LEDs mounted inside diffuse spheres on the shaft of the instrument. This allows Micron to perform basic tremor suppression and motion-scaling functionalities. See Figs. 15.1 and 15.2 for the setup.

15.2.1 Problem Definition

The ASAP measurement system provides very fine positioning information of the instrument and allows for general tremor compensation via filtering in the

frequency domain. However, it has no knowledge of what an operator sees in the microscope. Thus, the current Micron system cannot attempt to keep the tip aligned with a vein or to maintain a safe distance from anatomical features. The core issue addressed here is controlling the tip of Micron based on observations made with a stereo camera to effect three behaviors: snap-to, motion scaling, and standoff regulation.

The first behavior, snap-to, involves guiding the Micron tip to a 3D point in space and maintaining the tip at that location. Snap-to can be thought of as a more constrained version of tremor suppression and is useful when the tip must be held stable, e.g., for injections. The second behavior, motion scaling, is more practical when very precise movements are needed. Every movement made by the operator is scaled by a user-defined factor, thus reducing positioning errors. The finite range of the actuated tip limits when motion scaling can be applied, so it is only turned on when in the vicinity of the target. The final behavior, standoff regulation, serves as a preventative measure against accidental, unwanted contact. In this mode, Micron can attempt to avoid bringing the tip in contact with points by actively maintaining a preset distance from pre-defined "off-limits" areas. Each behavior has unique properties that can benefit a surgeon in different circumstances.

15.2.2 Visual Servoing

is a popular approach to guiding a robotic appendage or manipulator using visual feedback from cameras [9]. Given a target pose or position that the robot is to reach, the goal of visual servoing is to minimize the following error:

$$e(t) = s(m(t), a) - s^* \tag{15.1}$$

where s^* represents the desired positions, $s(m(t),a)$ the measured positions, $m(t)$ the measured feature points in the image, and a any external information needed (such as camera parameters). In general, $s(m(t),a)$ is usually the endpoint, or tip, of the manipulator. The tip position is determined from $m(t)$, the image coordinates of the tracked tip, and a, the camera mapping between world space and the image coordinates. In practice, s^* may not be known a priori and may instead be calculated from image features as well.

The approach used to minimize the error $e(t)$ can be done in one of two general ways: position-based visual servoing or image-based visual servoing [9, 10]. Image-based servoing uses an *image Jacobian* or *interaction matrix* to convert errors measured in the image directly into a velocity the robot should attempt to maintain. In contrast, position-based servoing treats the camera system as a 3D position sensor and measures the error in the task space rather than in the image. In the case of controlling only the translation of a tool, as is the case with the 3-degree-of-freedom (3DOF) Micron micromanipulator, it has been shown that these two approaches are equivalent [11]. Therefore, this research uses the position-based visual-servoing

approach because of the well-defined positioning system provided by ASAP and the ability to run calibration routines online. Furthermore, implementing the standoff regulation requires distance metrics in 3D space.

15.2.3 Novelty Considerations

Micron has unique characteristics that differentiate the system from a typical visual-servoing setup. First, Micron is not a fully autonomous robot, in that it has a limited range of motion whose reach is determined by the user holding the micromanipulator. The operator may move Micron to a position where the tip of the instrument cannot reach the target. Second, an external measurement system is available which allows for online calibration of the system, either before each run or during the run. Third, unlike a purely closed-loop system, Micron has to account for human dynamics involving the human eye-hand coordination feedback loop. Other research, mainly [12], explicitly considers control by a human user in micromanipulation, but only for the purposes of high-level task sharing and direction. For the majority of this paper, interaction with the human controller will not be explicitly considered, so as to give a more complete characterization of the system's performance in the context of visual servoing.

These novel problems must be eventually resolved, and thus the results will be evaluated and discussed with these considerations in mind.

15.3 System Design

ASAP and Micron are integrated on a real-time LabVIEW® target machine with the ASAP measuring system running in parallel with the controller. The Micron interface and the vision system run on a standard Windows® PC that is networked to the real-time machine to retrieve ASAP positioning information, perform stereo visual servoing, and send control signals back to Micron.

15.3.1 Visual Feedback

Designed for microsurgical work, Micron is operated under a high-power Zeiss OPMI® one microscope with a magnification often exceeding 25× and a visual workspace often only several millimeters in diameter. Two PointGrey Flea2 cameras capturing 800 × 600 video at 30 Hz are mounted to the microscope, providing a stereo view of the workspace. Each camera view is approximately 2 × 3 mm with each pixel corresponding to ∼3.4 μm.

The micromanipulator tip and feature landmarks are tracked in both views, giving a stereo reconstruction of the instrument tip relative to the targets. Since advanced tracking is not the topic of this research, the tip and target are marked with different colored paint for easy visual identification. Tracking is performed with a simple but robust color tracker [13]. The highly optimized and popular Intel® OpenCV library is used for implementing the computer vision techniques.

15.3.2 Micromanipulator Control

The chief control problem is how to use visual servoing in the context of Micron; in other words, given the tracked tip and target position, how can a control signal be derived in world, or ASAP, coordinates? To do so, an understanding of how camera coordinates relate to 3D world ASAP coordinates is needed. The fundamental perspective camera equation is $p = MP$, where P is a 4×1 homogenous point in 3D world coordinates that is projected to p, a homogenous 3×1 image coordinate by the 3×4 camera matrix, M. M is derived in the following section and defines the projective mapping between ASAP and the cameras. A second camera observes the same point P, creating a joint observation system defined by the fundamental perspective camera equation for each camera: $p_1 = M_1 P$ and $p_2 = M_2 P$. These equations can be combined and solved using the homogenous linear triangulation method described in [14]. Thus, as seen in Fig. 15.3, each set of the 2D points in the stereo pair will yield an acceptable back-projected 3D point.

Now that the tracked tip and target image locations have been reconstructed as 3D points in the ASAP workspace, the goal is to drive the error $E = P_{tip} - P_{target}$ to zero by controlling the endpoint velocity of the tip. When the error is zero, the tip and target should be coincident. The velocity can be determined as a proportion λ of the error:

$$v - \lambda(P_{tip} - P_{target}) \tag{15.2}$$

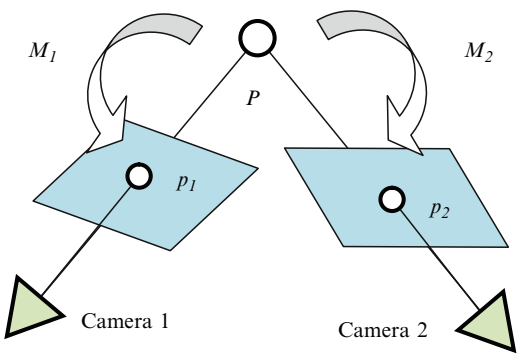

Fig. 15.3 Multiple view camera geometry, showing the projective relationship M_1 and M_2 that map the 3D point P to image coordinates p_1 and p_2 viewed by two cameras. Note that this is for the general case; the camera views in the Micron setup are parallel

Because velocities command the motion of the tip, errors due to errors in the calibration are absorbed with each new velocity calculation and drive E asymptotically to zero even in the presence of calibration errors.

15.3.3 Calibration

Currently, control of Micron operates in the coordinate system defined by the ASAP measurement system. However, the control signals are derived from the tracked tip and target viewed in the stereo camera setup. Furthermore, any preoperative information is usually registered in the image reference system. Thus calibration mappings M_1 and M_2, for cameras 1 and 2 respectively, are needed to transform from pairs of 2D image coordinates p_1 and p_2 to a 3D world coordinate point P.

In visual servoing, only the rotation mapping is important as translation is handled by streaming many sequential velocities to guide the tip in the direction of the target. However, because ASAP provides very accurate positions of the tip in 3D world coordinates, the full perspective mapping can be obtained. Furthermore, the full perspective camera mappings are useful because they can provide the visual trackers a rough estimation of where the tip is in the image. This reduces the amount of processing time required to locate the tip in the image, yielding increased framerates and better control performance.

A corresponding set of 3D world coordinates P_i and 2D image coordinates p_{1i} and p_{2i} form an over-determined system of equations $p_{1i} = M_1 P_i$ and $p_{2i} = M_2 P_i$, which can be solved by $M_1 = p_1 P^+$ and $M_2 = p_2 P^+$ where P^+ denotes pseudo-inversion. A method that is more robust is the Direct Linear Transformation algorithm [14]. This yields the pinhole camera perspective parameters, allowing a two-way mapping between 2D stereo image coordinates and 3D ASAP coordinates.

Calibration can be performed online, using the first 5–60 s of corresponding world and image coordinates in each run. If system positioning, magnification, and focus do not change between runs, calibrations may be reused, since the visual servoing does not require highly accurate absolute calibration [15], which is cumbersome to obtain with a microscope [16]. The calibration routine involves the operator moving the tip randomly through the workspace, including up and down. A typical 60-s calibration yields approximately 2,000 data points, from which outliers are automatically removed via a simple distance metric before the calibration calculations are performed. After calibration, the 3D tip position as measured by ASAP can be projected in the image accurately within 20 pixels and the tracked tip in the stereo images can be reconstructed in 3D space with an absolute mean error of $\sim$200 μm. Over time, the absolute calibration accumulates errors relative to ASAP as the tool pose is changed and the system shifts; however, this is not a problem as the control depends on the relative difference between the tip and target positions.

15.4 Experimental Results

Three different experiments were carried out to evaluate the desired behaviors of snap-to, motion-scaling, and standoff-regulation. First and foremost, the goal is to demonstrate the correctness and accuracy of each behavior. To eliminate any human-in-the-loop influences or disturbances, such as tremor, and achieve very repeatable results, all experiments requiring movement of the handheld micromanipulator were performed with the micromanipulator attached to the very precise (sub-μm) six-axis Polytec PI F-206.S HexAlign™ Hexapod manipulator. Since a machine will be "holding" Micron, it is equally important to evaluate the feasibility of applying these behaviors when a human is operating the micromanipulator. As such, a fourth experiment tested the helpfulness of the snap-to feature in a pointing task involving human tremor and compared it against basic tremor cancellation already implemented in Micron.

15.4.1 Experiment 1: Snap-to

Experiment 1 tested the snap-to functionality for convergence time and accuracy to a stationary point. Human hand motion and tremor are rapid, necessitating a fast response time. The experiment, seen in Fig. 15.4, servos the Micron tip to a 3D point defined by a colored needle tip. Both the micromanipulator and target point were held stationary. The target point on the needle was rigidly held by a clamp and Micron was firmly affixed to the Hexapod; only the Micron tip was actuated. Because the Hexapod was not actively moving the Micron handle, tremor reduction was not used for this experiment.

The experiment was performed from three different starting locations with three identical runs for each location. A summary of several important statistics is listed for each location in Table 15.1. First, the initial distance between the tip and target is listed, as this determines convergence time, i.e., the time required for the tip to converge on the target, where successful convergence is defined as being within

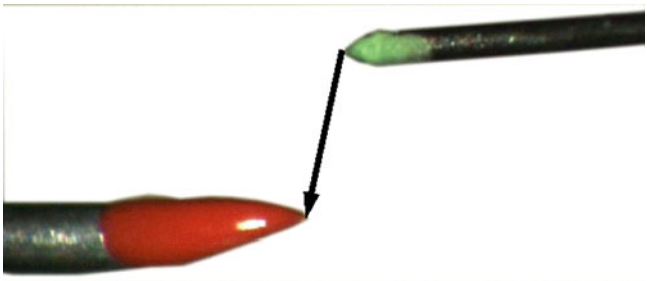

Fig. 15.4 Snap-to target experiment servoing green-color coded Micron instrument tip (200-μm diameter) to a stationary 3D target point defined by a red colored needle tip

Table 15.1 Speed and accuracy of servoing the tip to a 3D target from three different locations. Each location was reached three times to obtain a mean and standard deviation. RMSE measures the distance error between the tip and target for 15 s after convergence

Initial distance (μm)	Convergence Time (s)	Distance RMSE (μm)
375.3 ± 2.5	0.54 ± 0.02	16.6 ± 0.4
449.2 ± 5.6	0.59 ± 0.07	17.5 ± 0.4
677.9 ± 0.8	0.69 ± 0.04	18.3 ± 0.4

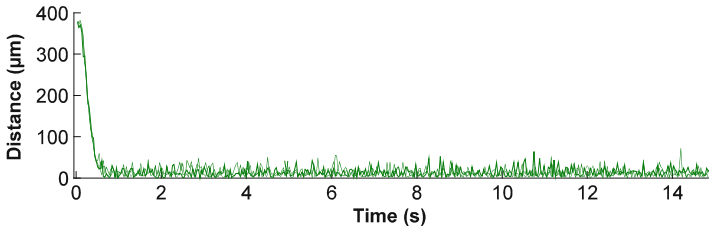

Fig. 15.5 Euclidean distance between Micron tip and target for three runs from the second location

25 μm of the target. Once the tip has converged, the RMSE is calculated from the 3D Euclidean distance between the tip and target during the 15 s after the target has been reached. Fig. 15.5 shows the distance error between the actuated Micron tip and the target for all three runs of the first location. The noise after convergence is caused mostly by small errors in the image trackers magnified by the backprojection into 3D. All runs exhibit similar trajectories and noise patterns.

While the convergence accuracy of the snap-to behavior is high, the convergence time of approximately half a second is rather long. Once converged, the visual servoing can hold a stationary point very well, even in the presence of disturbances. For example, if the whole Micron instrument is moved, it is desirable for the tip position to actuate fast enough that it can still remain steady on the target. If the response is too slow, tremor introduced as the human user operates will result in oscillations as the tip tries and fails to keep moving faster than tremor.

To model tremor-like movement, a disturbance signal was induced by moving the Hexapod base in all three dimensions and in a roughly sinusoidal pattern. This was done only with snap-to, and without any of the tremor-compensation techniques used by Micron. As shown in Fig. 15.6, the Micron tip remained steady even with rather large and rapid changes in position. This indicates that even in the case of rapid tremor motion, the Micron tip can remain "snapped-to" a stationary target very accurately. Experiment 4 expounds more by testing it with real tremor.

15.4.2 Experiment 2: Motion-Scaling

In experiment 2, the micromanipulator was moved at a constant speed in 3D space past the target point using the Hexapod micropositioner. When the tip of the

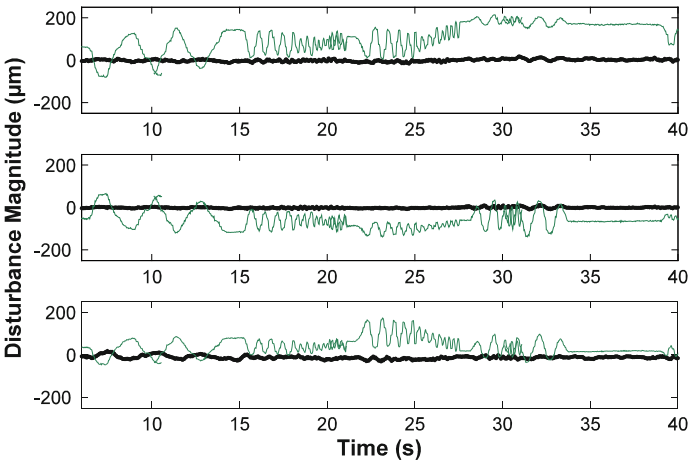

Fig. 15.6 Micron tip position (*thick black line*) snapped-to a target even with large, rapid changes in Micron instrument positioning (*thin green lines*) in X, Y, and Z directions (*top, middle, bottom* respectively)

Table 15.2 Mean measured 3D velocity before coming in range of the target, while the tip is within a 170 μm radius of the target, and after the tip has passed the edge of the circle. Three runs were executed for each scale tested: 1.5, 2, 3

Initial velocity (μm/s)	Scaled velocity (μm/s)	Final velocity (μm/s)	Measured scale
95.5 ± 1.9	62 ± 0.1	96.4 ± 0.7	1.5 ± 0.0
91.6 ± 4.6	43.9 ± 4.0	91.7 ± 8.4	2.1 ± 0.1
95.3 ± 1.0	30.6 ± 0.2	96.9 ± 0.9	3.2 ± 0

instrument was detected to be within an arbitrarily chosen 170-μm radius of the target, the motion-scaling behavior was activated with a scale factor of 1.5, 2, or 3. Thus the constant velocity of the tip should be reduced by a factor of $1/s$ while the tip is in vicinity of the target. The variability from $1/s$ was examined to determine the effectiveness of this technique. As seen in Table 15.2, the motion scaling works very well. There is a slight difference between the desired scale and the actual scale, but the overall variability is low. Velocity variability from time instant to time instant is influenced by the noise level and is difficult to assess accurately. Figure 15.7 shows the slope of the position and the numerically-differentiated velocity (smoothed with a 1 Hz lowpass filter).

15.4.3 Experiment 3: Standoff-Regulation

Experiment 3 validates the ability of the visual-servoing controller to maintain a standoff distance from a 3D target point. In this case, instead of snapping-to, the

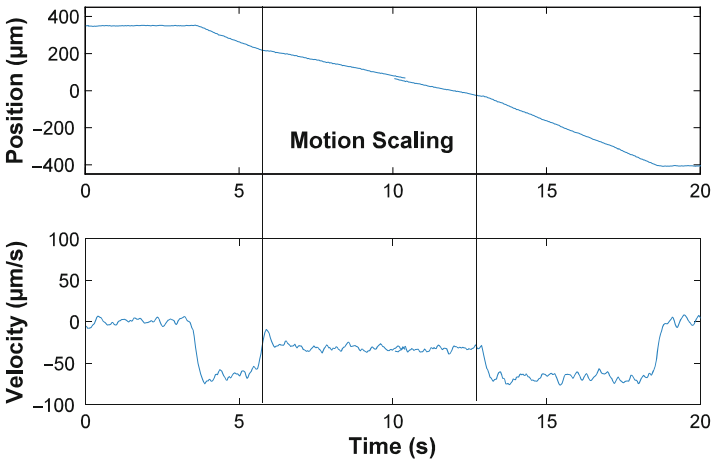

Fig. 15.7 Position and velocity of the Micron tip from one run as the instrument is moved with constant velocity. The middle motion-scaling region represents when the tip is within range of the target

desired action is for the tip to avoid the target. This could be useful in many surgical situations where "keep-away" points or zones might be defined to avoid unwanted and possibly harmful contact with tissue. As with the motion scaling, a spherical volume is defined around the target point in 3D. If the tip comes within 240 µm of the target, a repulsive force is exerted on the tip to guide it away. In this simple example, the repulsive field is modeled after a charged particle; thus the force exerted on the tip is always away from the center of the target. The Hexapod micropositioner is used to move the Micron tip in a straight line approaching the target at three different offset distances. The resulting trajectories can be viewed in Fig. 15.8. The standoff-regulation does push the trajectory of the tip away from the target. Additionally, the trajectory that clearly did not come near the target was unaffected. This simplistic model of a charged particle can be modified to maintain a constant standoff.

15.4.4 Experiment 4: Pointing Task

One common task in micromanipulation is pointing, or keeping the tip steady at some target. Sustained injection of a drug or chemical agent, for example, may be the purpose. To enhance accuracy in this task, it is necessary not only to suppress the "neurogenic" tremor component at 8–12 Hz [17], but also to suppress lower-frequency components as well. One way to accomplish this is to know the target point about which the user is trying to keep the tip steady. Experiment 4 compares a human operator attempting a pointing task unaided, with frequency-based tremor compensation, and with the snap-to image guidance. One subject performed three

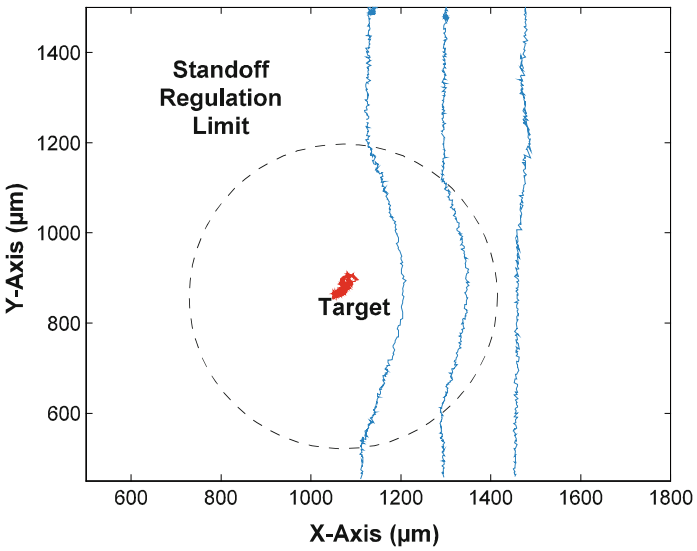

Fig. 15.8 Three tip trajectories, two of which infringe the repulsive field and are therefore pushed away from their paths to maintain separation between the target and the tip

Table 15.3 RMSE distance between the target and Micron tip during a 60-s pointing task

Unaided (µm)	compensation (µm)	Snap-to (µm)
222.9 ± 61.3	175.8 ± 65.9	70.1 ± 25.9

runs for each scenario, attempting to keep the Micron tip steady at the 3D target position for 60 s. The evaluation metric is the RMSE between the target point and the Micron tip. Table 15.3 lists the results. As expected, frequency based tremor compensation performed better than unaided. The snap-to performed even better, although the error was much higher than reported earlier because Micron could not always reach the target point.

15.5 Discussion and Conclusion

We present techniques for vision-based guidance of an active handheld micromanipulator, which yield encouraging initial results in a challenging environment. Using a stereo vision setup with a simple calibration routine, Micron employs visual servoing to increase accuracy in pointing tasks, even over existing tremor-cancellation methods. In a stationary pose, we have shown that finer motor control is possible locally around a target using motion scaling, and a surgeon can define "keep-away" areas to help avoid unwanted tissue contact. A demonstration of Micron with these three behaviors can be viewed in the video accompanying this paper.

One issue not dealt with is the finite manipulator range. If Micron is snapping-to, the user easily can shift the entire manipulator out of range of the target. Because the actuators can only move a finite amount before reaching their limits, additional behavior is needed to compensate. Additionally, to be useful in a completely handheld situation such as a surgical procedure, the controller will need to resolve conflicts between the user's movements and the activated behaviors. For instance, it may be more important to observe the "keep-away" constraints and not damage tissue than to maintain a motion-scaling behavior.

As future work, we plan on developing more realistic ways to track targets and surgical instruments, thereby obviating the current reliance of color tracking. Because magnification and focus can change during an operation, future work will include online routines that detect these changes and update the calibration accordingly through adaptive gains. As for the controller, a more sophisticated control algorithm is needed for standoff regulation. Evaluation work will move toward testing of these behaviors in more realistic settings.

Acknowledgments This work was supported in part by the National Institutes of Health (grant no. R21 EY016359), the American Society for Laser Medicine and Surgery, the ARCS Foundation, and a National Science Foundation Graduate Research Fellowship.

References

1. Mitchell, B., Koo, J., Iordachita, I., Kazanzides, P., Kapoor, A., Handa, J., Hager, G., Taylor, R.: Development and application of a new steady-hand manipulator for retinal surgery. In: IEEE International Conference on Robotics and Automation, pp. 623–629 (2007)
2. Fleming, I., Voros, S., Vagvolgyi, B., Pezzementi, Z., Handa, J., Taylor, R., Hager, G.: Intraoperative visualization of anatomical targets in retinal surgery, In: IEEE Workshop on Applications of Computer Vision (2008)
3. Berger, J.W., Madjarov, B.: Augmented reality fundus biomicroscopy a working clinical prototype. Arch. Ophtalmol. **119**, 1815–1818 (2001)
4. Li, X., Zong, G., Bi, S.: Development of global vision system for biological automatic micromanipulation system. IEEE Int. Conf. Robot. Autom. **1**, 127–132 (2001)
5. Yamamoto, H., Sano, T.: Study of micromanipulation using stereoscopic microscope. IEEE Trans. Instrum. Meas. **51**, 182–187 (2002)
6. Riviere, C.N., Ang, W.T., Khosla, P.K.: Toward active tremor canceling in handheld microsurgical instruments. IEEE Trans. Robot. Autom. **19**, 793–800 (2003)
7. Zhang, Z.: A flexible new technique for camera calibration. IEEE Trans. Pattern. Anal. Mach. Intell. 1330–1334 (2000)
8. MacLachlan, R.A., Riviere, C.N.: High-speed microscale optical tracking using digital frequency-domain multiplexing. IEEE Trans. Instrum. Meas. 58(6), 1991–2001 (2008)
9. Chaumette, F., Hutchinson, S.: Visual servo control, part I: basic approaches. IEEE Robot. Autom. Mag. **13**, 82–90 (2006)
10. Hutchinson, S., Hager, G.D., Corke, P.I.: A tutorial on visual servo control. IEEE Trans. Robot. Autom. **12**, 651–670 (1996)
11. Hespanha, J.P., Dodds, Z., Hager, G.D., Morse, A.S.: What tasks can be performed with an uncalibrated stereo vision system? Int. J. Comput. Vis. **35**, 65–85 (1999)

12. Ammi, M., Ferreira, A.: Involving the operator in the control strategy for intelligent tele-micromanipulation. In: IEEE/ASME International Conference on Advanced Intelligent Mechatronics, p. 2 (2003)
13. Yang, M.H., Ahuja, N.: Gaussian mixture model for human skin color and its application in image and video databases. In: Proceedings of the SPIE Storage and Retrieval for Image and Video Databases, vol. **3656**, pp. 458–466 (1999)
14. Hartley, R., Zisserman, A.: Multiple View Geometry in Computer Vision. Cambridge University Press, Cambridge (2003)
15. Hager, G.D.: A modular system for robust positioning using feedback from stereovision. IEEE Trans. Robot. Autom. **13**, 582–595 (1997)
16. Danuser, G.: Photogrammetric calibration of a stereo light microscope. J. Microsc. **193**, 62–83 (1999)
17. Elble, R.J., Koller, W.C.: Tremor. Johns Hopkins, Baltimore (1990)